scientific reports

Check for updates

OPEN

Paleoenvironmental reconstruction of the Middle Ordovician Majiagou Formation in the northeastern Ordos Basin and its effect on organic matter enrichment

Yiran Wang[1], Xiaofeng Wang[1]✉, Wenhui Liu[1,2], Tao Zhang[2] & Dongdong Zhang[1]

The alteration of paleoenvironment is a crucial factor influencing the variations in hydrocarbon-forming organisms and the preservation of organic matter. This study focuses on the marine carbonate rocks of the Middle Ordovician Majiagou Formation located in the Daniudi area of the northeastern Ordos Basin. By analyzing major, trace, and rare earth element concentrations alongside carbon and oxygen isotope composition characteristics, we reconstructed the paleoenvironment and examined its impact on organic matter enrichment. The findings indicate that carbonate minerals are predominantly developed within the Majiagou Formation, which exists primarily in a suboxic-anoxic environment. Furthermore, paleotemperature data for seawater reveals a gradual upward trend that aligns with global seawater temperature changes from the Darriwilian to Dapingian stages of the Middle Ordovician. There are differences in the paleoenvironment of the Majiagou Formation in the northeastern part of the basin in different periods, which is an important factor affecting the enrichment of organic matter. The paleoenvironment during the deposition of the first member of the Majiagou Formation is more conducive to the enrichment of organic matter and is an effective source rock development interval.

Keywords Marine carbonate, Paleoenvironmental reconstruction, Organic matter enrichment, Majiagou Formation, Ordos Basin

With the deepening of oil and gas exploration, deep marine oil and gas has become one of the important exploration areas. The Ordos Basin is the second largest sedimentary basin on land in China, and the Paleozoic marine strata contain abundant oil and gas resources, making it an important layer for natural gas exploration in the Ordos Basin. After more than 30 years of exploration and development, important breakthroughs have been made in the exploration of natural gas in subsalt carbonate rocks of the Ordovician Majiagou Formation. Subsalt dolomite gas reservoirs have been discovered, forming natural gas enrichment areas such as Daniudi and Shenmu[1–3]. However, the effective source rocks of Ordovician subsalt natural gas reservoirs are still unclear. The Ordovician Pingliang Formation calcareous shale has a certain hydrocarbon generation capacity, but the distribution and scale are relatively limited. Although the Upper Paleozoic coal-bearing strata have considerable hydrocarbon generation capacity, it is difficult for hydrocarbons to migrate to the subsalt strata due to the barrier of the thick gypsum strata of the Majiagou Formation. The subsalt carbonate strata of the Ordovician Majiagou Formation in the Ordos Basin have the characteristics of high evolution degree and low TOC. It is controversial whether it can become an effective source rock and contribute to the Ordovician natural gas reservoir. Liu et al.[4] found fluorescent asphalt and fluorescent organic inclusions in carbonate rocks of Majiagou Formation by laser-fluorescence microscopy system. Sun et al.[5] used the methods of source rock desorption gas carbon isotope-natural gas carbon isotope to clarify that the Paleozoic oil-type gas in Daniu underground is mainly derived from the source rock of the Lower Paleozoic Majiagou Formation. Liu et al.[6] pointed out that the contribution of Lower Paleozoic hydrocarbon sources in different regions of Ordos Basin is different, and the contribution of Lower Paleozoic hydrocarbon sources of pre-salt natural gas reservoirs in the central and eastern parts of the

[1]State Key Laboratory of Continental Evolution and Early Life, Department of Geology, Northwest University, Xi'an 710069, Shaanxi, China. [2]Petroleum Exploration and Production Research Institute, SINOPEC, Beijing 100083, China. ✉email: wangxf@nwu.edu.cn

basin cannot be ignored, and there are effective hydrocarbon sources in Lower Paleozoic. Wang et al.[7] pointed out that the process and amount of hydrocarbon generation experienced by highly evolved carbonate source rocks cannot be negated by low TOC, and factors such as the type and number of hydrocarbon generating organisms, the composition of organic carbon isotopes and the negative drift of inorganic carbon isotopes should be comprehensively considered. These studies show that the marine carbonate rocks of the Ordovician Majiagou Formation in the Ordos Basin are one of the effective source rocks in the basin and have important exploration value.

The Ordovician is one of the key periods of biological macroevolution since the Phanerozoic. The marine biodiversity has increased dramatically and the ecosystem is more complex, which is the 'Ordovician biological radiation'[8]. At the same time, the biological radiation event was accompanied by strong paleoenvironmental changes[8]. The change of paleoenvironment and climate may be an important factor affecting biological evolution[9–11], which in turn affects the abundance and preservation conditions of buried organic matter during the sedimentary period. Therefore, the study of Ordovician paleoenvironment is particularly important.

The large natural gas fields discovered in the Ordos Basin are mainly distributed in the northern part of the basin. Previous studies have systematically studied the oil and gas geology in this area[12–15], but there are relatively few studies on the paleoenvironmental evolution of the Ordovician Majiagou Formation. Therefore, strengthening the study of paleoenvironmental reconstruction in the northern Ordos Basin has important guiding significance for clarifying the enrichment law of organic matter in the Ordovician strata. This paper selects the Daniudi gas field in the northeastern Ordos Basin as the research area, and conducts a comprehensive study of petrology and geochemistry of the Majiagou Formation, including mineral and maceral content analysis, major and trace element analysis, TOC and inorganic carbon and oxygen isotope analysis. From the aspects of redox conditions, basin properties, paleoclimate and paleotemperature, and compared with the global Ordovician seawater paleotemperature changes, the paleoenvironmental changes during the sedimentary period of the Ordovician Majiagou Formation in the northeastern part of the basin and their effects on organic matter enrichment were discussed in detail.

Geological setting

The Ordos Basin is located in the central and western regions of China and is a multi-cycle composite superimposed craton basin. It belongs to the secondary tectonic unit of the North China platform. Its tectonic and sedimentary evolution is controlled by the Xingmeng Trough in the north and the Qinqi Trough in the southwest. It has the characteristics of internal relative stability and peripheral activity, and is one of the most stable tectonic units in China, containing abundant oil and gas resources[16,17] (Fig. 1). The sedimentary environment is mainly controlled by the L-type central paleo-uplift, and the craton on the eastern side of the paleo-uplift is in the epicontinental sea environment[18,19].

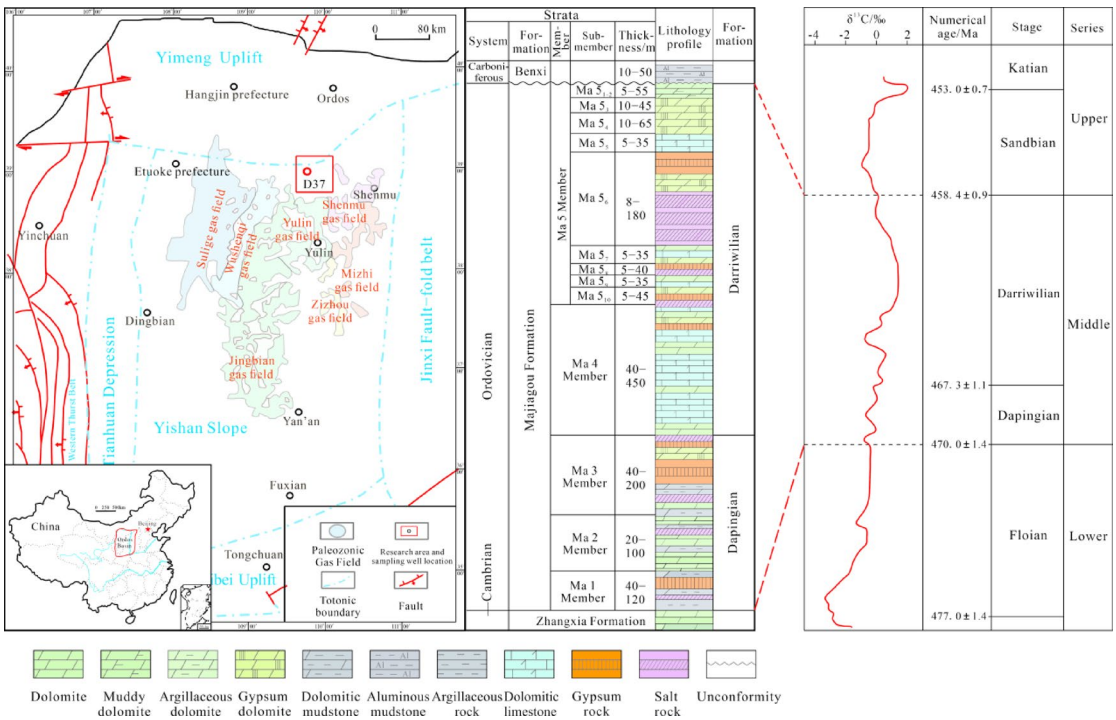

Fig. 1. Map showing the structural location and strata development of the research area in the Ordos Basin. D37 is the well for collecting core samples in this article (the geochronological frame modified from Ref.[23–25]; The international standard Ordovician profile on the right is from Ref.[26]).

In the Ordovician, the central paleo-uplift located in the Etuokeqi-Dingbian-Qingyang area divided the Ordos Basin into Qilian Sea area, Qinling Sea area and North China Sea area, and controlled the sedimentary differentiation of the Ordovician in the west, south and east. The Lower Ordovician Yeli, Liangjiashan and Majiagou Formations are developed in the central and eastern part of the basin. The paleotectonic framework of ' alternating uplift and depression ' in the eastern part of the central paleo-uplift controls the Ordovician Majiagou Formation to develop a set of carbonate rocks and gypsum-salt rocks. The lithologic association has obvious cyclicity in the vertical direction and can be divided into six lithologic sections from the first member of the Majiakou Formation to the sixth member of the Majiakou Formation (abbreviated as Ma1 to Ma 6) from bottom to top[15,20,21]. The sedimentary period of Ma 1, Ma 3 and Ma5 is a regressive period, which is dominated by salt rock and gypsum rock, with carbonate rock interlayers. The sedimentary period of Ma2, Ma4 and Ma6 is transgression period, and the lithology is mainly limestone and dolomite. The Majiagou Formation is generally a gypsum-salt-carbonate rock series[22].

The Majiagou Formation in the Ordos Basin belongs to the Middle Ordovician of the Lower Paleozoic. According to the standardized sequence stratigraphic division scheme and the lithofacies paleogeographic characteristics of the Majiagou Formation, combined with previous studies on the Ordovician sequence stratigraphy and biostratigraphy of the Ordos Basin[23–25], this paper corresponds the sedimentary period of the Majiagou Formation to the Middle Ordovician Daruiweier Stage and the Daping Stage (Fig. 1).

Materials and methods

Sample information

The samples analyzed in this paper are from the drilling core of D37 well in Wulanchabu area, northeastern Ordos Basin. The samples are distributed in Ma1 and Ma 3 to Ma 5. According to different depth intervals, a total of 62 core samples were sampled. Among them, the lithologies of Ma 5 samples are limestone, limestone dolomite and gypsum dolomite, the lithologies of Ma 4 samples are limestone and gypsum dolomite, and the lithologies of Ma 3 and Ma 1 samples are gypsum dolomite and gypsum bearing argillaceous dolomite. Microscopic identification shows calcite is generally anhedral and dolomite euhedral, which, together with hand-sample observation and 5% HCl testing (calcite reacts vigorously), provides diagnostic criteria for distinguishing these carbonate minerals. According to the experimental requirements, the samples were crushed and ground to 80–120 mesh and 200 mesh sizes under non-polluting conditions for major and trace element analysis, TOC analysis, carbon and oxygen isotope analysis, and X-ray diffraction analysis. In order to study the petrological characteristics of the samples, the cores of different layers were observed by optical microscope.

Methods

Microscopic observation

Twenty-four samples were selected for microscopic observation by Nikon Eclipse LV100N POL microscope. All samples were made into polarized light slices from vertical slices according to China's oil and gas industry standard SY/T 5913-2004. All observations are carried out under plane polarized light (PPL). Minerals and biological components are identified according to the SY/T 5368-201X standard. Microscopic observations were performed at the State Key Laboratory of Continental Dynamics at Northwest University.

Major and trace earth element analyses

Under non-polluting conditions, the fresh samples were ground to 200 meshes. The main elements were analyzed by X-ray fluorescence spectrometry on the RIX2100 system, and the concentration of the main elements was analyzed with an accuracy of more than 5%. The operation steps met the Chinese national standard GB/T 14506.28-2010. The trace elements and rare earth elements were analyzed by Thermo Fisher ELEMENT XR inductively coupled plasma mass spectrometry (ICP-MS). The analysis of trace elements conforms to the national standard GB/T 14506.30-2010, and the precision is higher than 5%. Major and trace earth element analyses were performed at ALS Testing (Guangzhou) Co., Ltd.

Inorganic carbon and oxygen isotope analysis

The carbon and oxygen isotope test of the sample was analyzed by GasBench II multi-purpose sample preparation device and Thermo Finnigan MAT253 Plus isotope ratio mass spectrometer. After all the samples were ground to 200 mesh powder, about 0.3 mg of the sample was reacted with phosphoric acid at 70 °C for 2 h, and helium was used as the carrier gas. The CO_2 gas was continuously flowed through the CombiPAL automatic sampler into the isotope ratio mass spectrometer for analysis. The chromatographic column was a PoraPbtQ chromatographic column of 25 m × 0.32 mm produced by Agilent, USA. During the experiment, two standard samples were placed for each 12 samples. The sample analysis results were calibrated by the Chinese national standard sample GBW04405, and the standard deviations were less than 0.08‰ (using VPDB as the standard), and the data repeatability was good. Carbon and oxygen isotope analyses were performed at the Stable Isotope Geochemistry Laboratory of the State Key Laboratory of Continental Dynamics at Northwest University.

X-ray diffraction analysis

X-ray diffraction analysis was performed using an Ultima IV X-ray diffractometer. The sample with a size of 200 mesh was placed in a sample holder and the surface of the powder sample was smoothed and tested by an X-ray diffractometer. The resolution of the X-ray diffractometer is higher than 60%, and the comprehensive adjustment is better than ± 1%. The analysis procedure followed the Chinese oil and gas industry standard SY/T 5163-2010. X-ray diffraction analysis were performed at the Conventional Rock and Mineral Properties Analysis Laboratory at Northwest Institute of Eco-Environment and Resources (NIEER), Chinese Academy of Sciences (CAS).

Total organic carbon determination

For carbonate rock samples, total organic carbon analysis needs to remove the carbonate components in the sample first. The specific operation is as follows: take 100–200 mg sample powder (particle size is 200 mesh), add it to the permeable crucible and weigh it accurately, and then add sufficient dilute hydrochloric acid (volume ratio of concentrated hydrochloric acid to deionized water is 1:7) to dissolve carbonate minerals. After standing at room temperature for 12 h, the crucible is heated in a water bath at 80 °C for 3 h to ensure the complete removal of carbonate minerals. The crucible is then thoroughly washed with deionized water and the sample is dried in an oven at 100 °C. After that, ELTRA CS800 carbon and sulfur analyzer was used for determination. Total organic carbon determinations were performed at the Carbon and Sulfur Analysis Laboratory of the State Key Laboratory of Continental Dynamics at Northwest University.

Results

Petrological characteristics

The results of thin section identification show that the Majiagou Formation in the study area is mainly carbonate rock and evaporite. The clastic rock is mainly developed in Ma 1. Carbonate minerals are mainly calcite and dolomite and limestone with different grains (mainly micrite and powder crystal) (Fig. 2a, b). Calcite or quartz are filled in dissolution pores (Fig. 2c, d), and bioclastic and quartz nodules are distributed in micrite dolomite (Fig. 2e). The clastic particles are mainly quartz and a small amount of feldspar, which are scattered in the mud in an angular shape (Fig. 2f).

A total of 15 core samples from Ma 1 and Ma 3 to Ma 5 in well D37 were selected for XRD analysis. The results show that the main minerals of marine carbonate rocks in Majiagou Formation are calcite and dolomite. The average contents of calcite and dolomite (carbonate minerals) are 28.9% and 46.8%, respectively. Detrital minerals, including clay minerals, quartz, orthoclase and plagioclase, are mainly distributed in Ma 1, and only a small amount is distributed in other layers. Anhydrite and pyrite are present in Ma 1 carbonate, with an average content of 27% and 2.47%, respectively. The mineral content of carbonate samples is shown in Fig. 3.

Characteristics of major and trace elements

The elements analyzed in this study include major oxides (Al_2O_3, CaO, etc.; Table 1) and trace elements (Ba, Co, Ce, etc.; Table 2). Compared with the upper continental crust (UCC)[27], there are obvious losses of Al_2O_3, Fe_2O_3, K_2O and obvious enrichment of CaO and MgO in Ma 3 to Ma 5. The obvious losses of Al, Fe and other elements indicate that there are less terrigenous clastic materials in Ma 3 to Ma 5, which are mainly dominated by the chemical deposition of carbonate rocks. In contrast, there are relatively more terrigenous clastic materials in Ma 1 (Fig. 4a). Compared with the post-Paleozoic Australian shale (PAAS)[27,28], the Mo and U of the Majiagou Formation are relatively depleted. At the same time, Ma 1 is more enriched in lithophile elements such as Sc and Th and rare earth elements such as Ce, La and Co compared with Ma 3 to Ma 5 (Fig. 4b). It also shows that there are more terrestrial materials during the deposition of Ma 1.

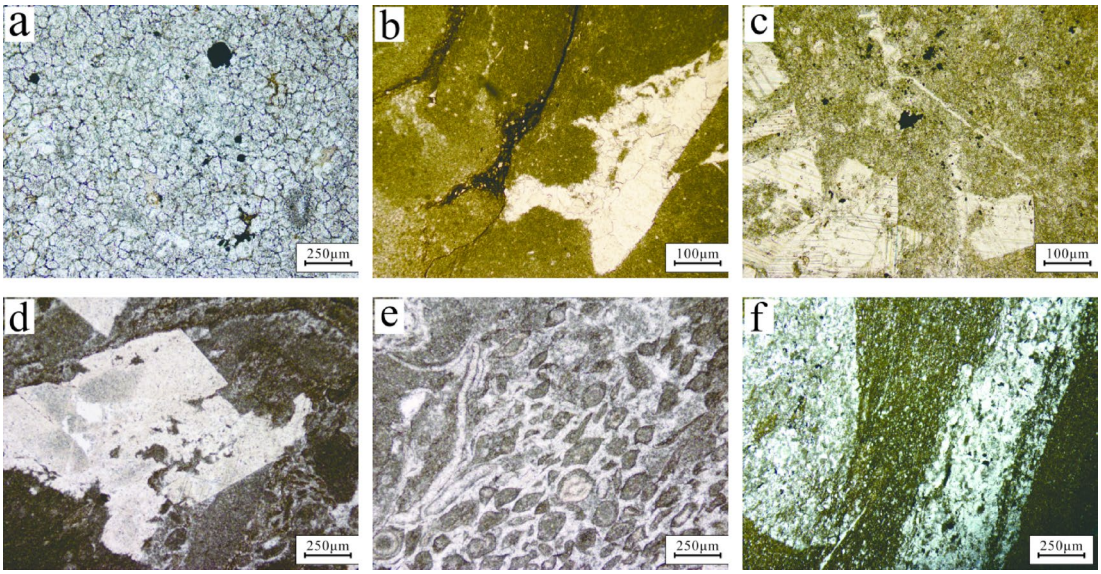

Fig. 2. Core petrological characteristics of D37 well in the northeastern margin of the basin [(**a**) pelitic dolomite containing pyrite, Ma 5, 2901.9 m; (**b**) Mud crystal limestone, dissolved pore filling calcite, Ma 5, 2955.3 m; (**c**) Microfractured micritic limestone, dissolved pore filling calcite, Ma 4, 3049.6 m; (**d**) bioclastic argillaceous dolomite containing quartz nodules, Ma 3, 3218.2 m; (**e**) salty gypsiferous argillaceous dolomite, dissolved pore filling quartz, Ma 3, 3220.34 m; (**f**) Detrital micritic anhydrite, Ma 1, 3374.7 m)].

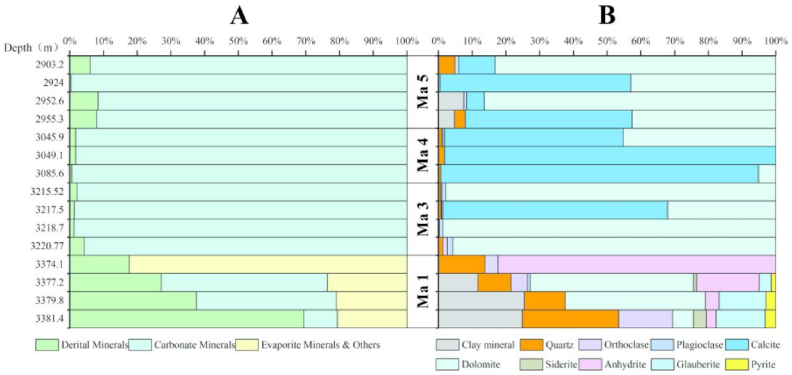

Fig. 3. Mineral contents of the marine carbonate rocks from the Majiagou Formation [(**A**) Mineral compositions are divided into three categories: detrital minerals, carbonate minerals and evaporite minerals & others; (**B**) Mineral compositions are displayed as the XRD analysis result].

	Al_2O_3	CaO	TFe_2O_3	K_2O	MgO	MnO	Na_2O	P_2O_5	SiO_2	TiO_2	LOI 1000
Ma 5(20)	0.06–23.24	3.06–54.3	0.07–3.17	0.02–7.01	0.98–18.85	–	0–0.16	0–0.21	0.28–49.87	0.01–1.24	7–45.24
Ma 5_{avg}	2.64	37.48	0.77	0.78	9.74	–	0.03	0.02	7.52	0.13	39.67
Ma 4(13)	0.1–0.48	44.1–55.1	0.03–0.19	0.08–0.26	0.27–8.53	–	–	–	0.78–1.9	–	42.9–43.96
Ma 4_{avg}	0.25	52.27	0.09	0.16	2.31	–	–	–	1.41	–	43.42
Ma 3(12)	0.04–5.17	19.8–51.8	0.11–1.27	0.08–3.21	2.93–21	–	0.01–2.08	0–0.06	0.67–21.2	0.01–0.21	31.8–46.85
Ma 3_{avg}	1.85	27.86	0.68	1.17	17.39	–	0.24	0.02	7.74	0.07	40.35
Ma 1(17)	0.29–17.3	0.85–34.5	0.34–5.44	0.19–9.9	2.75–9.51	0.01–0.03	0.15–4.47	0.01–0.17	1.06–57.6	0.02–0.79	4.46–16.66
Ma 1_{avg}	11.09	12.34	3.36	6.55	5.80	0.02	0.57	0.09	39.00	0.47	9.84
UCC	15.17	4.19	4.49	3.39	2.2	0.07	3.89	0.2	65.89	0.5	

Table 1. Major oxides content interval and average value (%). The value in brackets is the number of samples, and this line of data represents the range from the minimum value to the maximum value; The avg represents the average value; the symbol '–' indicates that the content is less than 0.01; the UCC value is quoted from Ref.[27].

TOC and inorganic carbon and oxygen isotope composition

The TOC and carbon and oxygen isotope compositions of the Majiagou samples from Well D37 were tested (Table 3). The results show that the $\delta^{13}C$ value is distributed in − 8.3‰ ~ 0.1‰, and the $\delta^{18}O$ value is distributed in − 10 to − 4.5‰. TOC has the characteristics of marine carbonate rocks and is generally low, distributed in 0.007 to 0.6%. The $\delta^{13}C$ values of the Ma 3 to Ma 5 are distributed in the range of − 4.7‰ ~ 0.1‰, which is basically consistent with the $\delta^{13}C$ value distribution of the international standard Ordovician profile. The $\delta^{13}C$ value of the Ma1 is distributed in the range of − 8.3 to 4.7‰, which is significantly negative compared with the $\delta^{13}C$ value (-1‰ ~ 0‰) of the Daping stage of the international standard Ordovician profile (Fig. 1). The average $\delta^{18}O$ values of Ma 1, Ma 3 to Ma 5 are − 5.49‰ − 5.53‰ − 7.3‰ and − 9‰, respectively, showing a gradually decreasing trend. The samples with higher TOC values are mainly concentrated in the first member of Ma, and the highest value can reach 0.6%.

Discussion

Redox-sensitive elements refer to the fact that the solubility of elements in water is obviously controlled by the oxidative environmental conditions of water, mainly including Mo, U, V, Ni, Co and other elements. In the process of changing redox conditions, the occurrence state of these elements will change[29]. The elements of sedimentary rocks are mainly derived from four aspects, including terrestrial input, seawater deposition, biological deposition and hydrothermal sources. It is generally believed that only the element content of seawater deposition and biological deposition can indicate redox conditions. On the other hand, diagenesis and metamorphism also have a great influence on redox analysis. Therefore, it is necessary to exclude the influence of terrestrial input, hydrothermal fluid, diagenesis and metamorphism before using element index to distinguish redox conditions[29–33].

During the deposition process, the elemental composition of carbonate rocks is easily affected by non-carbonate components (such as clastic materials). In order to remove the interference of these factors in the analysis process, it is necessary to evaluate the degree of influence of the debris in the sample. Th and Sc are used to track terrestrial inputs, as terrestrial detrital minerals often contain concentrations of Th and Sc that are tens of times higher than those of pure carbonates[34–36]. In addition, the composition of rare earth elements in carbonate rocks is easily affected by non-carbonate components such as clastic input[37,38]. Therefore, parameters

	Ce	Co	Cr	La	Mo	Ni	Sc	Sr	Th
Ma 5(20)	2.2–133.5	0.5–16.1	0.2–140	1.1–76.2	0.05–1.4	0.1–37.7	0.2–14.1	67.7–140.5	0.21–38.6
Ma 5_{avg}	18.417	2.415	10.93	10.065	0.32	4.457	2.035	111.985	4.2245
Ma 4(13)	1.5–2.98	0.6–1	–	0.7–1.5	0.2–0.73	0.12–1.5	0.2–0.5	150.5–347	0.21–0.6
Ma 4_{avg}	2.10	0.75	–	1.02	0.42	0.70	0.36	231.96	0.39
Ma 3(12)	2.4–20.3	0.6–4.8	0.2–20	1.1–10.8	0.17–1.65	0.8–10.7	0.2–5	88.8–9740	0.16–6.38
Ma 3_{avg}	10.14	2.02	6.08	4.78	0.85	4.40	1.83	1806.92	2.22
Ma 1(17)	6.5–120.5	0.9–21.1	0.2–90	2.3–61.6	0.14–2.59	0.6–47.9	0.4–17.7	96.7–1975	0.37–20.6
Ma 1_{avg}	69.36	11.42	58.78	35.36	0.71	25.59	9.36	603.60	10.72
PAAS	80	10	110	35	1	55	16	200	14.6
	U	**V**	**Hf**	**Zr**	**Ba**	**Mn**	**P**	**Pb**	**Mn/Sr**
Ma 5(20)	0.27–14	0.5–144	0.1–6.9	1–33	1.4–291	23–99	20–1060	0.4–16.2	
Ma 5_{avg}	2.0985	16.825	0.9	28.6	43.51	58.2	153.5	4.063636	0.52
Ma 4(13)	0.29–0.97	1–3	–	2–5	2.1–27.5	9–20	10–30	0.5–2.5	
Ma 4_{avg}	0.54	2.08	–	3.00	9.07	12.69	15.45	1.47	0.05
Ma 3(12)	0.57–2.16	3–42	0.1–1	2–43	7.5–493	15–81	10–310	1.7–8.2	
Ma 3_{avg}	1.43	14.67	0.40	14.83	125.98	54.33	96.67	3.50	0.03
Ma 1(17)	0.16–5.5	3–122	0.1–10.5	2–381	8.9–572	37–184	30–760	0.9–23.1	
Ma 1_{avg}	2.74	77.65	3.10	114.70	311.30	107.59	412.94	9.84	0.18
PAAS	3.1	150							

Table 2. Trace element content range and average (10^{-6}) and related parameters. The value in brackets is the number of samples, and this line of data represents the range from the minimum value to the maximum value; The avg represents the average value; the symbol '–' indicates that the content is less than 0.01; the PAAS value is quoted from Ref.[27,28].

such as ΣREEs less than 12 ppm, Y / Ho greater than 26, Ti less than 0.5%, Al less than 1%, Th, Zr and Hf less than 20 ppm can be used to evaluate whether the sample is contaminated by detrital components[38–40]. In addition, the formation of carbonate rocks mainly undergoes a chemical deposition process, and the Sc content is less (less than 2 ppm) than that of clastic rocks. As shown in Tables 1, 2 and 3, the samples in this study (Al_{avg} = 2.27%, Ti_{avg} = 0.11%, Th_{avg} = 4.81 ppm, Sc_{avg} = 3.7 ppm, Zr_{avg} = 44.17 ppm, Hf_{avg} = 1.3 ppm) are only slightly affected by terrestrial input of detrital materials. The sample data can be used to indicate the paleoenvironment of the Majiagou Formation in the study area.

In addition, in order to reduce the influence of carbonate on the different dilution degree of sediments[41], the enrichment coefficient EF is usually used to indicate the enrichment degree of trace elements in sedimentary water[31]. The formula is as follows (Table 4):

$$\mathrm{EF}_{\mathrm{element}} = \frac{(\mathrm{element}/\mathrm{Al})_{\mathrm{sample}}}{(\mathrm{element}/\mathrm{Al})_{\mathrm{PAAS}}} \quad (1)$$

where Element and Al represent the content of a certain element and Al in the sample. The samples were normalized by PAAS (post-Archean Australian shale)[28]. If $X_{EF} > 1$, it indicates that the element is enriched relative to the average marine shale, $X_{EF} > 3$ is obviously enriched, $X_{EF} > 10$ is moderately-strongly enriched, and on the contrary, $X_{EF} < 1$ indicates relative loss[42,43,78].

The Fe and Mn in carbonate rocks are very sensitive to metamorphism and post-diagenesis, and are generally enriched[44]. Although rare earth elements can generally maintain their characteristics under metamorphism, under high temperature and high water–rock ratio conditions, a large amount of loss of rare earth elements, loss of Ce and enrichment of Eu often occur[45]. Therefore, if there is a negative correlation between Fe and Ce and between Mn and Ce, it indicates that the samples are affected by metamorphism and post-diagenesis. However, this correlation was not found in this study (Fig. 5), and the effects of metamorphism and post-diagenesis were excluded.

Strong diagenesis may cause changes in the elemental composition of rocks, which in turn affects the paleoenvironmental information reflected by the elemental composition. Elements such as Mn and Sr can be used as empirical reference values to indicate the degree of influence of diagenesis on carbonate rocks and evaporites. Studies have shown that when $\omega(Mn)/\omega(Sr) \leq 0.6$, rock samples are not or less affected by diagenesis. The element information in the sample can be used as a geochemical indicator to indicate the ancient sedimentary environment[46,47]. The $\omega(Mn)/\omega(Sr)$ of the rock samples of the Majiagou Formation used in this study is generally less than 0.6 (Table 2), indicating that the samples have not been or have been less affected by diagenesis. The results of elemental analysis can be used to reflect the paleoenvironmental characteristics of the Majiagou Formation in the study area.

The redox environment is a comprehensive reflection of the deposition rate and hydrodynamic conditions. Generally, the anoxic environment is more conducive to the preservation of organic matter and is closely

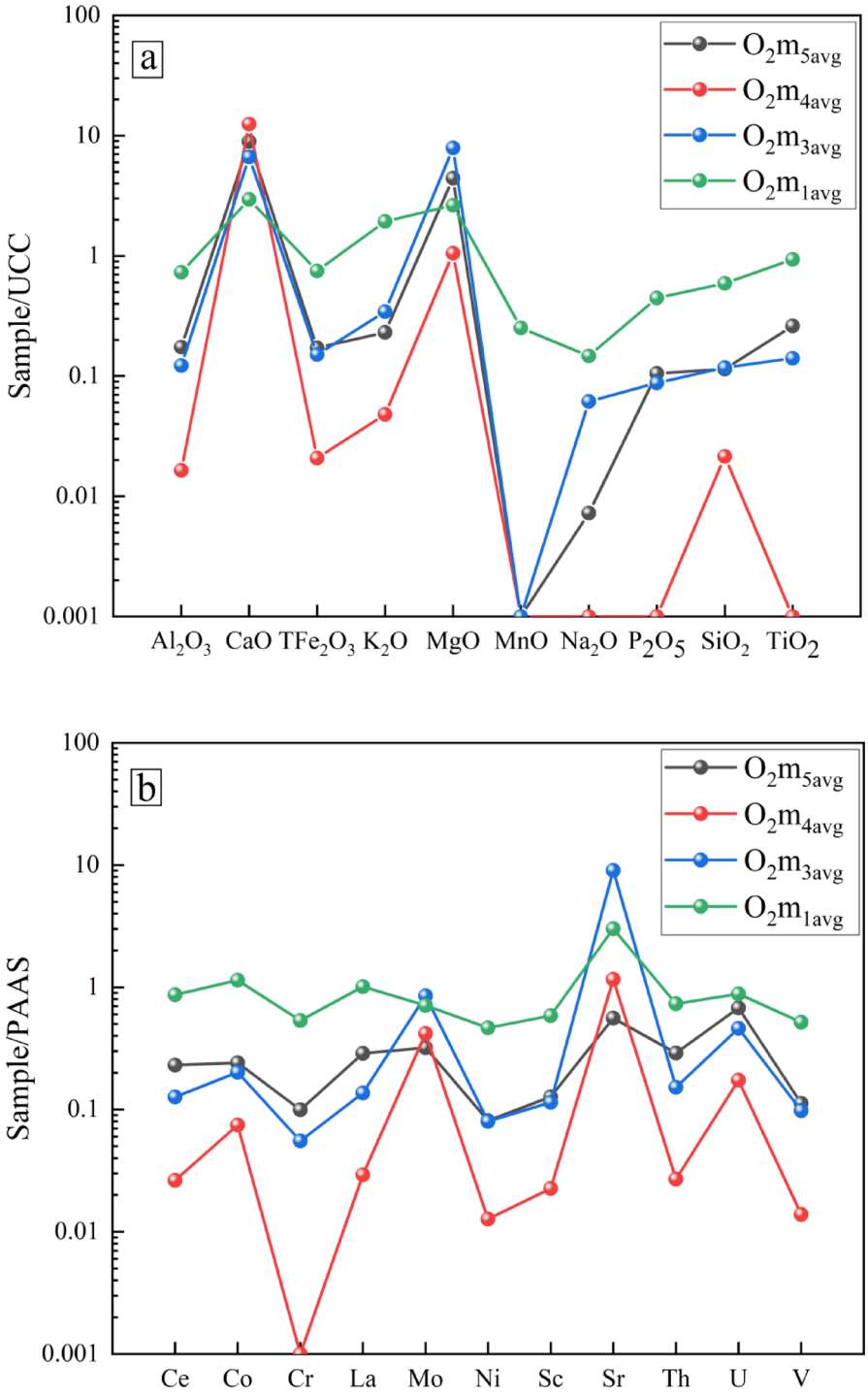

Fig. 4. (**a**) Major oxides spider diagram normalized to upper continental crust (UCC); (**b**) Trace elements spider diagram normalized to the post-Paleozoic Australian shale (PAAS).

related to the formation of source rocks[48,49]. Redox sensitive elements refer to the fact that the solubility of elements in water is obviously controlled by the oxidation environment of water, including Mo, U, V, Ni, Co and rare earth elements (REE), which have been widely used in the study of the evolution and reduction state of formation water during the sedimentary period[50]. However, the changes in these elements are influenced by various geological factors, and when conducting research on redox conditions, multiple discriminant indicators should be comprehensively considered. Based on the applicability of various parameters, this study selected seven relatively stable and accurate ratio parameters of Mo, U, V, Ni, Th, La and Ce to compare the changes of paleoenvironment[38,51,52,54].

	Al (%)	Ti (%)	CIA	C value	TOC (%)	$\delta^{13}C_{carb}$ (‰)	$\delta^{18}O_{carb}$ (‰)
Ma 5(20)	0.03–12.3	0.04–0.77	60–78.34	0.001–0.23	0.007–0.29	−4.7 to −0.6	−10 to −8.3
Ma 5_{avg}	1.40	0.08	73.39	–	0.12	−1.78	−9
Ma 4(13)	0.05–0.25	–	50–63.16	–	0.13–0.2	−0.5 to 0.1	−7.8 to −6.8
Ma 4_{avg}	0.13	–	56.77	–	0.16	−0.12	−7.3
Ma 3(12)	0.02–2.43	0.01–0.14	46.03–62.01	0.002 to 0.03	0.1–0.39	−2.6 to 0	−7.6 to −5
Ma 3_{avg}	0.98	0.04	51.68	–	0.20	−0.73	−5.53
Ma 1(17)	0.15–9.16	0.01–0.47	37.18–64.15	0.02 to 0.3	0.11–0.63	−8.3 to −4.7	−6.6 to −4.5
Ma 1_{avg}	5.87	0.28	58.33	–	0.24	−6.38	−5.49

Table 3. The range and average value of Al content, Ti content, TOC, $\delta^{13}C$ value and $\delta^{18}O$ carb value and related parameters. The value in brackets is the number of samples, and this line of data represents the range from the minimum value to the maximum value; The avg represents the average value; the symbol ' – ' indicates that the content is less than 0.01.

	Co_{EF}	Cr_{EF}	Ni_{EF}	V_{EF}	Mo_{EF}	U_{EF}
O2m5(20)	0.94–25.19	0.1–1.03	0.13–3.71	0.48–2.01	0.36–34.63	3.52–27.42
O2m5_{avg}	5.8	0.35	0.67	0.93	7.69	10.15
O2m4(13)	3.94–13.22	–	0.14–2.45	0.79–1.33	11.81–124.67	9.52–18.89
O2m4_{avg}	6.49	–	1.09	1.11	37.32	13.90
O2m3(12)	1.48–28.33	0.04–0.86	0.59–6.87	0.83–9.44	2.01–495.83	2.27–121.86
O2m3_{avg}	5.00	0.43	1.47	1.81	61.54	19.41
O2m1(17)	1.46–5.86	0.12–1.01	0.64–1.13	0.78–1.3	0.21–35.17	1.08–3.36
O2m1_{avg}	2.28	0.84	0.80	0.92	3.72	1.73

Table 4. Enrichment factors of Co, Cr, Ni, V, Mo and U in the study area. The value in brackets is the number of samples, and this line of data represents the range from the minimum value to the maximum value; The avg represents the average value; the symbol '–' indicates that the content is less than 0.01.

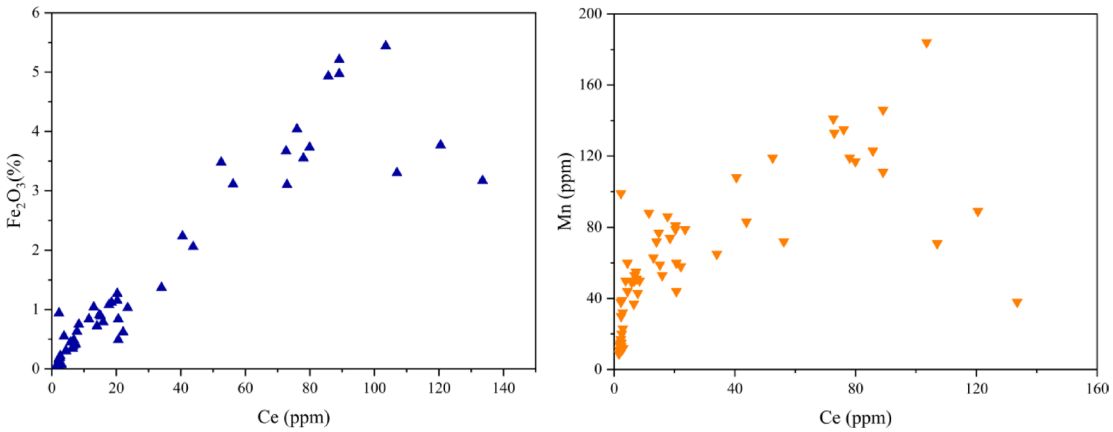

Fig. 5. Fe_2O_3-Ce correlation diagram and Mn-Ce correlation diagram.

It is not accurate to simply use the absolute content of trace elements to judge the redox conditions of water bodies. Therefore, the ratio of trace elements is often used as an indicator of the redox environment. The U/Th and V/(V/Ni) values of trace elements are widely used to analyze the evolution of paleoredox conditions[38,51,52]. The study of element ratio for redox conditions is mostly obtained from the study of clastic rocks. In carbonate rocks, due to the dilution effect, the content of trace elements is relatively low, and the boundary value of redox should be adjusted accordingly. Prasanta and Sarada[38] believed that the V/(V/Ni) values in carbonate rocks are 0.3 and 0.5, and the U/Th ratios are 0.2 and 0.5, which are the boundary values of oxidation, dysoxic and anoxic conditions. Ce is a variable valence element in rare earth elements. Ce anomaly will occur under different redox conditions, so it can be used as a tracer for redox conditions in ancient oceans[53]. Bai et al.[54] studied the geochemical characteristics of rare earth elements in the Devonian anoxic sediments of South China and pointed out that the Ce anomaly can be replaced by the Ce/La ratio. The Ce/La ratios of 1.8 and 2 are equivalent

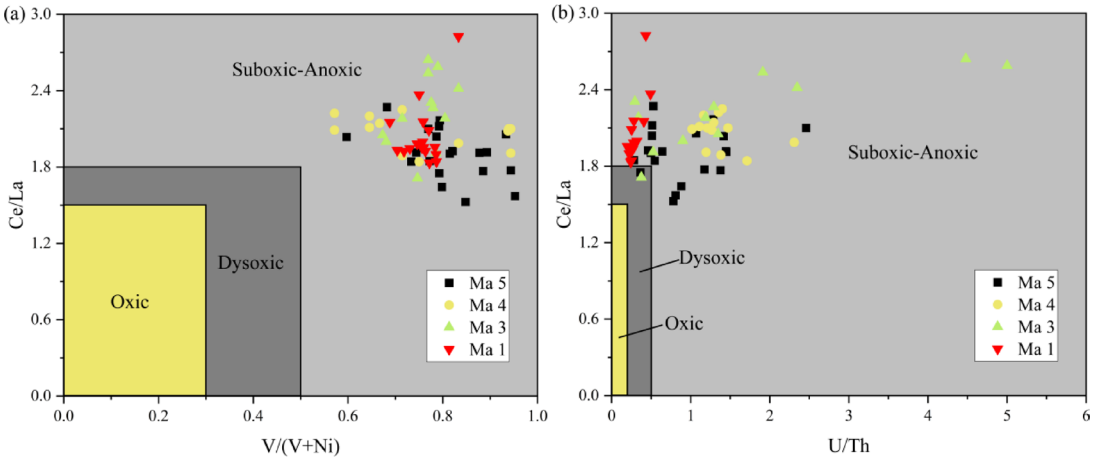

Fig. 6. The paleo-redox environment indicator map of the study area.

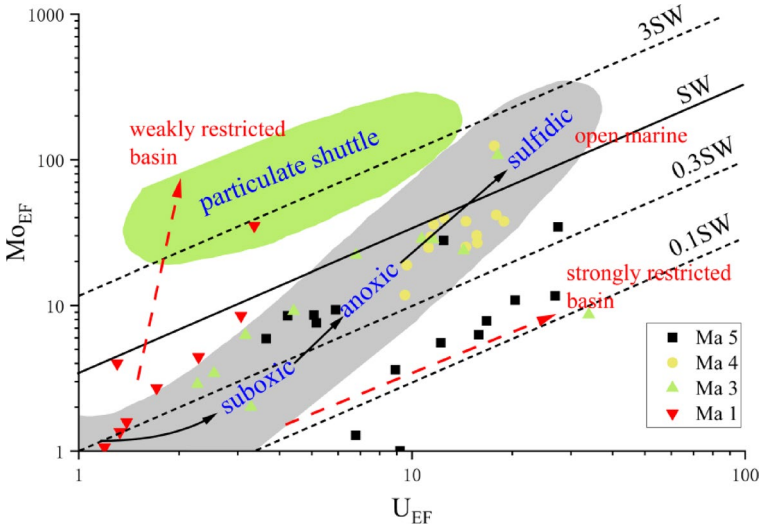

Fig. 7. U–Mo covariation diagram of Majiagou Formation samples in D37 well.

to the Ce anomaly values of −0.1 and 0, respectively. When Ce/La < 1.5, it is an oxygen-rich environment; when 1.5–1.8, it is a dysoxic environment; when it is greater than 2.0, it is a suboxic-anoxic environment. As shown in Fig. 6, except for a few samples of the Majiagou Formation in the study area are distributed in the dysoxic region, other data points are basically in the weak oxygen-anoxic region.

Geochemical analysis of Majiagou Formation samples reveals significant enrichment of Mo, U and Co, with Ni and V showing comparable enrichment levels to the Post-Archean Australian Shale (PAAS). The enrichment factors (EF) of Mo, U, Co, Ni and V display a bell-shaped trend from Ma 1 to Ma 5, peaking at intermediate stratigraphic levels. In contrast, Cr exhibits consistent depletion with progressively lower EF values upward through the section (Table 4). Mo and U are two relatively abundant valence elements in marine water. Piper and Perkins[29] found that the seawater contribution of Mo and U is 22 and 54 times that of biological contribution, respectively. The difference of their enrichment in sediments can be used to establish a U–Mo covariant model map to reflect the degree of redox in water and to reconstruct the basin[28,48,55]. From the U–Mo covariant model diagram (Fig. 7), it can be seen that Ma 1 is in a weak oxidation-anoxic weak retention environment, and Ma 4 is an open sea environment with deep anoxic water. The distribution of sample points in Ma 3 and Ma 5 is not concentrated. The reason for this distribution is that these two periods have experienced frequent sea level changes, resulting in changes in oxygen content in seawater.

In summary, the redox conditions of the Majiagou Formation in the northeastern part of the basin have not changed much during the sedimentary history, mainly in a suboxic-anoxic environment. The Ma 1 is in a suboxic-anoxic weak restricted environment. The Ma 4 is an open marine environment with deep anoxic water. The redox conditions of Ma 3 and Ma 5 have fluctuating changes, and the degree of environmental oxidation is relatively high.

The geochemical composition of sedimentary rocks will be affected by chemical weathering and sedimentary recycling. There are significant differences in the chemical alteration index (CIA) of clastic rocks under different climatic conditions. As the degree of chemical weathering increases and the climate becomes warm and humid, the reduction of free cation reaction will produce higher CIA values, the calculation formula is:

$$\mathrm{CIA} = 100 \times \mathrm{Al_2O_3}/\left(\mathrm{Al_2O_3} + \mathrm{Na_2O} + \mathrm{CaO^*} + \mathrm{K_2O}\right) \quad (2)$$

where CaO* only refers to CaO in silicate, according to the correction method adopted by Mclennan[56] : $\mathrm{CaO'} = \mathrm{CaO} - \frac{10}{3}\,\mathrm{P_2O_5}$, $\mathrm{CaO^*} = \mathrm{Min}(\mathrm{CaO'}, \mathrm{Na_2O})$.

The CIA value of unaltered rock is generally lower than 50, and the CIA value is between 50 and 65, reflecting weak chemical weathering under dry conditions. The CIA value is between 65 and 85, reflecting moderate chemical weathering under warm and humid conditions. The CIA value is between 85 and 100, indicating strong chemical weathering under humid conditions, and the CIA value of completely altered rock is 100[57,58]. However, metasomatism can change the content of unstable ions such as K^+ and Ca^{2+} in rocks and affect the accuracy of CIA. The Al_2O_3–($CaO^* + Na_2O$)–K_2O(A–CN–K) diagram is usually used to characterize the effect of metasomatism[58]. The rock is not affected by metasomatism or only weak metasomatism, and the weathering line of the sample will be parallel to the direction of A-CN or A-K[58,59]. In the A-CN-K diagram, the sample points of Ma1, Ma 3 and Ma 5 are distributed along the A-CN direction, indicating that the metasomatism of the samples is weak after the sedimentary period, and the CIA value can be used to determine the chemical weathering and paleoenvironment (Fig. 8). In the arid environment, strong evaporation and high alkalinity of water easily promote the precipitation of salt minerals, and Ca, Mg, Sr, Ba, K and Na are relatively enriched, while Fe, Mn, Cr, Ni, V and Co are relatively enriched in the humid environment. Therefore, the C value [Σ(Fe + Mn + Cr + Ni + V + Co) /Σ(Ca + Mg + Sr + Ba + K + Na)] can be used as an indicator to reflect the paleoclimate conditions[60,61]. This study comprehensively considers the common influence of C value and CIA, and reflects the paleoenvironment through the relationship between the above two. As shown in Fig. 9, the CIA value of the sample of Ma 1 in Da 37 well is 50.1–62.6, and the C value is between 0.02 and 0.3, indicating that Ma 1 was weakly chemically weathered during the deposition period, reflecting the arid to semi-arid and semi-humid climate; the CIA value of the samples in Ma 3 is 46–61.2, and the C value is between 0.002 and 0.03, indicating that Ma 3 was weakly chemically weathered during the deposition period, reflecting the arid climate; the CIA value of Ma5 samples is 60–78.1, and the C value is between 0.001 and 0.23, indicating that t Ma 5 samples suffered moderate chemical weathering during the sedimentary period, reflecting the semi-arid and semi-humid climate.

The $\delta^{18}O$ value of carbonate rock is an important index to reflect the oxygen isotope of water body during the sedimentary period. It is widely used in the reconstruction of paleotemperature during the sedimentary period, which is usually affected by the water temperature and diagenesis during the sedimentary period[62–64]. For the ancient marine carbonate rocks, the oxygen isotope index is greatly influenced by the later diagenesis. In general, oxygen isotope composition lighter than −10‰ is considered to be affected by diagenesis[65]. In this study, the $\delta^{18}O_{carb}$ of all samples is more than −10‰, which can be used to reflect the paleotemperature during the sedimentary period. According to Hays and Grossman[66] sea surface temperature formula:

$$\mathrm{T} = 15.7 - 4.36\left(\delta^{18}\mathrm{O_{carb}} - \delta^{18}\mathrm{O_{sw}}\right) + 0.12\left(\delta^{18}\mathrm{O_{carb}} - \delta^{18}\mathrm{O_{sw}}\right)^2 \quad (3)$$

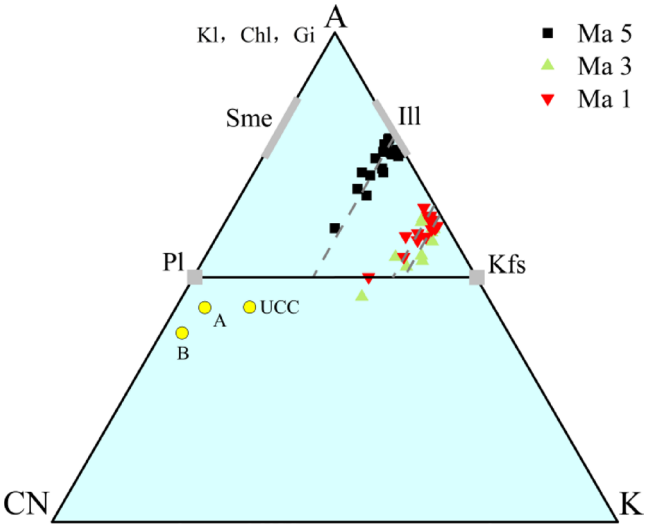

Fig. 8. A-CN-K ternary graph. (**A**) andesite; (**B**) basalt; Chl. chlorite; Ill. illite; Gi. gibbsite; Kfs. K-feldspar; Kl. kaolinite; Pl. plagioclase; Sme. Smectite; UCC. upper crust rocks. The dotted line is a trend line parallel to A-CN.

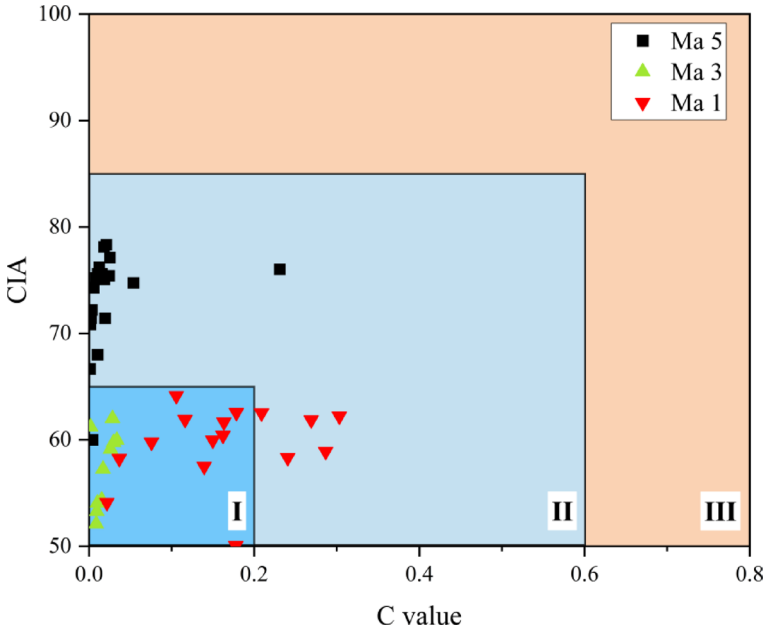

Fig. 9. The intersection diagram of CIA value and C value of D37 well in the northeastern part of the basin. I: arid climate; II: semi-arid and semi-humid climate; III: humid climate.

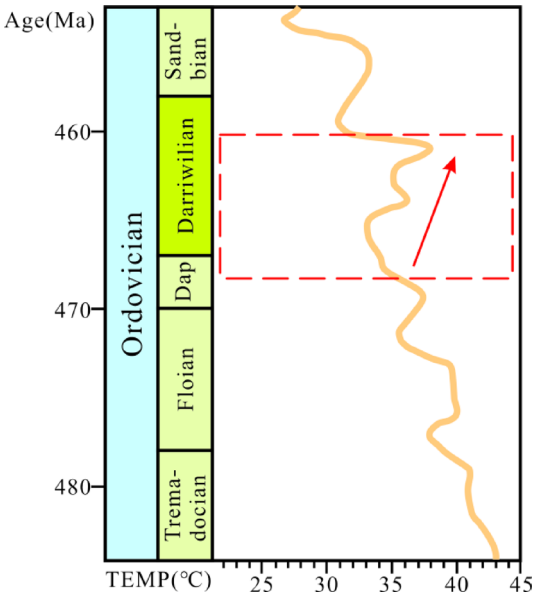

Fig. 10. Surface temperature of Ordovician seawater (Modified from Ref.[69]) The temperature rise from Darriwilian Stage to Dapingian Stage in the red dotted line frame is consistent with the conclusion of this study.

among them, the $\delta^{18}O$ value of the Middle Ordovician paleoseawater is about −6.6 to −4.0‰, and the average oxygen isotope composition of the sea water is set to 4.0‰[67,68]. Through the calculation of the oxygen isotope composition of the sample carbonate rock, this study shows that the seawater temperature of Ma 1, Ma 3 to Ma 5 is about 22.6 °C, 22.7 °C, 31.5 °C and 40.6 °C, respectively, and the seawater paleotemperature shows a gradual upward trend. This is consistent with the global change trend of seawater paleotemperature from Darriwilian Stage to Dapingian Stage of Middle Ordovician (Fig. 10)[69], and has a comparative significance with the Majiagou Formation in the northeastern Ordos Basin.

First of all, compared with other layers (Table 3, Fig. 11), the TOC value of Ma 1 member is higher, the average value of TOC is 0.24%, up to 0.63%, reaching the lower limit of TOC value (0.3% ~ 0.5%) of argillaceous effective source rock[70,71] and exceeding the lower limit of TOC value (0.1%) of marine carbonate hydrocarbon

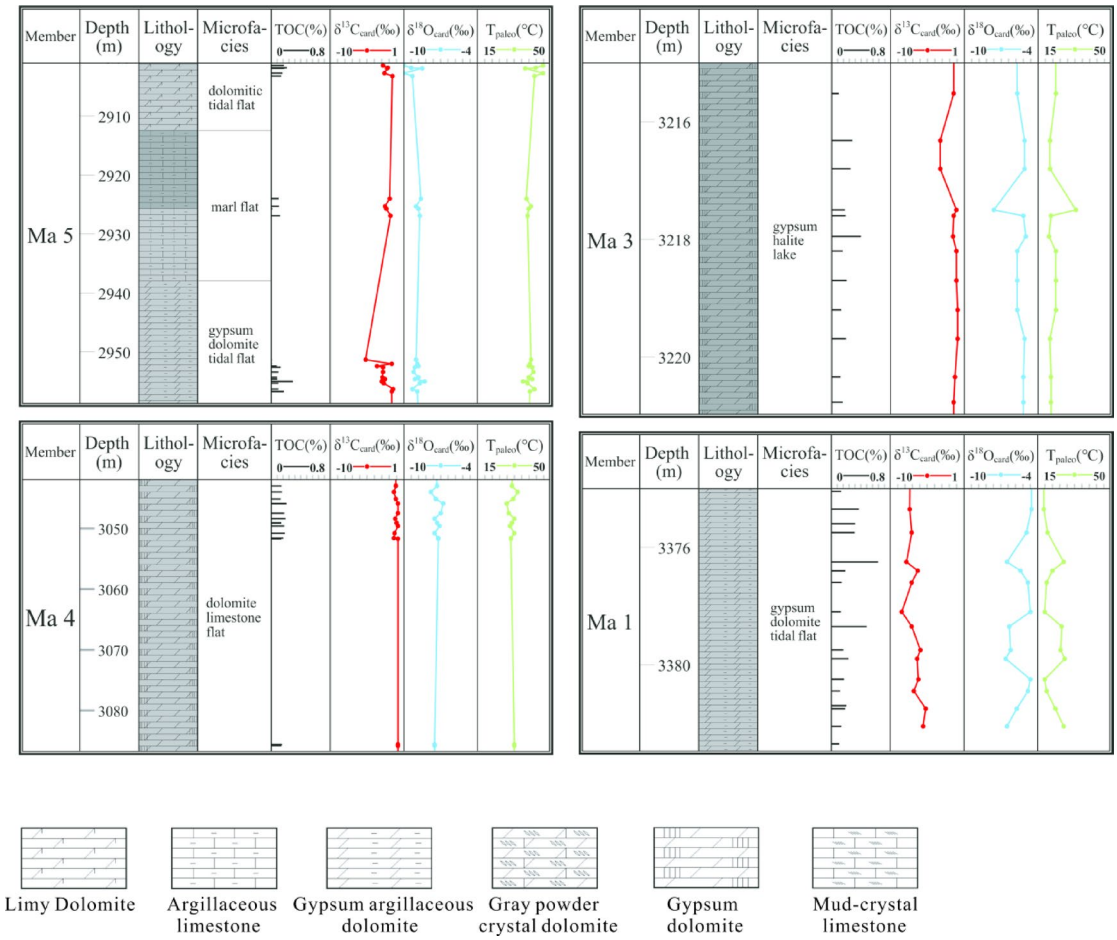

Fig. 11. Whole rock carbon and oxygen isotope signatures, paleotemperature signature and TOC contents of carbonate rocks in the different members of the Majiagou Formation in Well D37.

source[72]. In addition, the $\delta^{13}C$ value (−8.3‰ ~ 4.7‰) (Fig. 10) is significantly negative compared with the $\delta^{13}C$ value (−1‰ ~ 0‰) of the same period of the international standard Ordovician section. The factors causing the negative carbon isotope value of marine carbonate rocks in the Ordovician Majiagou Formation mainly include: (1) atmospheric freshwater leaching[73]; (2) Bacterial sulfate reduction (BSR)[74]; (3) Organic–inorganic interaction[6,75]. The formation of Ma 1 in the study area is deeply buried and located under the thick gypsum rock layer, and the formation temperature is higher in the higher mature stage[76], which is less affected by freshwater leaching and BSR. Therefore, the main reason for the negative shift of carbon isotope value of carbonate rocks in Ma 1 is organic–inorganic interaction, namely organic acid salt hydrocarbon generation and thermochemical sulfate reduction reaction (TSR)[6,75]. The TOC value and carbon isotope composition data have indicated that the carbonate strata of Ma 1 have higher paleoproductivity than other strata of the Majiagou Formation, and are favorable strata for organic matter enrichment.

The difference of paleoenvironment in each sedimentary period of Majiagou Formation is the main factor causing the differential accumulation of organic matter and the higher paleoproductivity of Ma 1. Suitable seawater temperature is conducive to the growth of marine organisms, while high temperature is not conducive to or even inhibits the reproduction and survival of marine organisms[69,77]. Ma 1 has a lower seawater temperature (22.6 °C), which is more conducive to the growth and prosperity of hydrocarbon generating organisms. At the same time, the sedimentation period of Ma 1 was in a weak restricted environment of weak oxidation and hypoxia, and the later stage was less affected by chemical weathering, which is conducive to the preservation of organic matter In summary, this paper believes that the carbonate rocks in the northeastern part of the basin are a favorable layer for organic matter enrichment compared with other layers, and have the potential to become an effective source rock.

Conclusion

From a petroleum geochemistry perspective, when employing elemental geochemical proxies to reconstruct paleoenvironmental conditions of deep marine carbonate source rocks, it is imperative to comprehensively evaluate potential interfering factors including detrital input, dilution effects, and diagenetic alterations. Current consensus holds that only those elements predominantly derived from seawater and biogenic sedimentation, with minimal post-depositional modifications, can serve as reliable paleoenvironmental indicators. Furthermore,

in assessing paleoproductivity of deep marine carbonate source rocks, the evaluation should incorporate not only residual total organic carbon (TOC) content but also account for hydrocarbon generation contributions from both organic–inorganic interactions such as organometallic complex catalysis and thermochemical sulfate reduction (TSR).

There are obvious differences in the paleoenvironment of Majiagou Formation in different periods in the northeast of the basin. Among them, Ma 1 is a suboxic-anoxic weak restricted environment, the seawater temperature is about 22.6 °C, and the degree of chemical weathering is weak, reflecting the arid to semi-arid and semi-humid climate ; Ma 3 and Ma 5 are suboxic-anoxic environment, and the seawater temperature is about 22.7 °C and 40.6 °C, respectively, which are subjected to weak and moderate chemical weathering, reflecting the arid to semi-arid and semi-humid climate. Ma 4 is an anoxic open sea environment with a sea temperature of about 31.5 °C. The seawater temperature during the deposition of the Majiagou Formation has a gradual upward trend, which corresponds to the trend of global seawater temperature change from the Darriwilian to Dapingian of the Middle Ordovician. Paleoenvironmental factors have an important influence on the enrichment of organic matter in the Majiagou Formation in the northeastern part of the basin. The lower seawater temperature in Ma 1 is more conducive to the prosperity of marine organisms. The suboxic-anoxic weak restricted environment during the deposition period and the weak chemical weathering degree in the later period provide good conditions for the preservation of organic matter. Therefore, the carbonate strata in Ma 1 have the potential to become effective source rocks.

Data availability

All data used in this study are provided in the manuscript in the main files as well as in the supplementary materials. Wang Yiran, one of the authors, can be contacted to access the X-ray technology-based mineral content data, his email is 427003112@qq.com.

Received: 19 February 2025; Accepted: 15 July 2025
Published online: 22 July 2025

References

1. Zhao, W. Z., Hu, S. Y., Liu, W., Wang, T. S. & Li, Y. X. Petroleum geological features and exploration prospect in deep marine carbonate strata onshore China: A further discussion. *Nat. Gas Ind.* **34**(4), 1–9. https://doi.org/10.3787/j.issn.1000-0976.2014.04.001 (2014).
2. Bao, H. P. et al. Hydrocarbon accumulation characteristics and exploration potential of Ordovician pre-salt formations by lateral hydrocarbon supply in the central-eastern Ordos Basin. *China Petrol. Expl.* **3**(25), 134–145. https://doi.org/10.3969/j.issn.1672-7703.2020.03.012 (2020).
3. Fu, J. H. et al. New discovery and favorable areas of natural gas exploration in the 4th Member of Ordovician Majiagou Formation by Well Mitan 1 in the eastern Ordos Basin. *Nat. Gas Ind.* **41**(12), 17–27. https://doi.org/10.3787/j.issn.1000-0976.2021.12.003 (2021).
4. Liu, D. H., Fu, J. H., Zhen, C. B., Xiao, X. M. & Mi, J. K. Research on hydrocarbon generation of Ordovician marine carbonatite of the Ordos Basin and genesis of Changqing Gas Fields. *Acta Geol. Sinica* **78**(4), 542–550. https://doi.org/10.3321/j.issn:0001-5717.2004.04.014 (2004).
5. Sun, X. et al. Evaluation of geochemical characteristics and source of natural gas in Lower Paleozoic, Daniudi area, Ordos Basin. *Petrol Geol. Exper.* **43**(2), 307–314. https://doi.org/10.11781/sysydz202102307 (2021).
6. Liu, W. H. et al. Restudy on geochemical characteristics and genesis of Jingbian gas field in Ordos Basin. *J. Northw. Univer. (Nat. Sci. Edn.)* **52**(6), 943–956. https://doi.org/10.16152/j.cnki.xdxbzr.2022-06-004 (2022).
7. Wang, X. F. et al. Hydrocarbon generation characteristics and evaluation methods of highly maturity carbonate source rocks. *J. Northw. Univer. (Nat. Sci. Edn.)* **52**(6), 957–967. https://doi.org/10.16152/j.cnki.xdxbzr.2022-06-005 (2022).
8. Wu, R. C., Calner, M., Lehnert, O., Perterffy, O. & Joachimski, M. M. Lower-Middle Ordovician $\delta^{13}C$ chemostratigraphy of western Baltica (Jämtland, Sweden). *Palaeoworld* **24**(1–2), 110–122. https://doi.org/10.1016/j.palwor.2015.01.003 (2015).
9. Haq, B.U., & Schutter, S.R. A chronology of Paleozoic sea-level changes. Science, **322**(5898), 64–68 (2008). https://www.jstor.org/stable/20144943.
10. Young, S. A., Saltzman, M. R., Ausich, W. I., Desrochers, A. & Kaljo, D. Did changes in atmospheric CO_2 coincide with latest Ordovician glacial-interglacial cycles?. *Palaeogeogr. Palaeoclimatol. Palaeoecol.* **296**, 376–388. https://doi.org/10.1016/j.palaeo.2010.02.033 (2010).
11. Pohl, A., Donnadieu, Y., Hir, G. L., Buoncristiani, J. F. & Vennin, E. Effect of ordovician paleogeography on the (in)stability of the climate. *Climate Past* **10**(6), 2053–2066. https://doi.org/10.5194/cp-10-2053-2014 (2014).
12. Wei, X. S. et al. Gas exploration potential of tight carbonate reservoirs: A case study of Ordovician Majiagou Formation in the eastern Yi-Shan slope, Ordos Basin, NW China. *Petrol. Explorat. Dev.* **44**(3), 319–329. https://doi.org/10.11698/PED.2017.03.01 (2017).
13. Lei, T. et al. Depositional model of the lower-middle Ordovician Majiagou Formation in Daniudi Gas Field, Ordos Basin. *J Paleogeogr.* **22**(3), 523–538. https://doi.org/10.7605/gdlxb.2020.03.036 (2020).
14. Wang, L. L., Fu, Y. & Fang, S. J. Elemental geochemical characteristics and geological significance of Majiagou Formation, eastern Ordos Basin. *Petrol. Geol. Exp.* **40**(4), 519–525. https://doi.org/10.11781/sysydz201804519 (2018).
15. Yu, Z. et al. Natural gas accumulation models and favorable exploration areas of the Cambrian-Ordovician in the Ordos Basin. *Nat. Gas. Ind.* **44**(8), 44–57. https://doi.org/10.3787/j.issn.1000-0976.2024.08.004 (2024).
16. Zhu, X. M. et al. Sedimentary characteristics and model of shallow braided delta in large-scale lacustrine: An example from Triassic Yanchang Formation in Ordos Basin. *Earth Sci. Front.* **20**(2), 19–28 (2013).
17. Fu, J. H. et al. Breakthrough and significance of natural gas exploration in the fourth member of Majiagou Formation of subsalt Ordovician in Ordos Basin. *China Petrol. Explor.* **27**(2), 47–58. https://doi.org/10.3969/j.issn.1672-7703.2022.02.005 (2022).
18. Guo, Y. Q. et al. Sedimentary systems and palaeogeography evolution of Ordos Basin. *J. Palaeogeogr.* **21**(2), 293–320. https://doi.org/10.7605/gdlxb.2019.02.017 (2019).
19. Li, W. H. et al. Sedimentary evolution of the late Paleozoic in Ordos Basin and its adjacent areas. *J. Palaeogeogr.* **23**(1), 39–52. https://doi.org/10.7605/gdlxb.2021.01.003 (2021).
20. Hou, F. H. et al. Depositional environment model of middle ordovician majiagou formation in ordos basin. *Marine Origin Petrol. Geol.* **7**(1), 38–45 (2002).
21. Shi, J. A. et al. Lithofacies paleogeography and sedimentary environment in ordovician majiagou formation eastern ordos basin. *Nat. Gas Geosci.* **20**(3), 316–324 (2009).

22. Fu, J. H. et al. New understandings of the lithofacies paleogeography of the middle assemblage of Majiagou Fm in the Ordos Basin and its exploration significance. *Nat. Gas. Ind.* **37**(3), 9–16. https://doi.org/10.3787/j.issn.1000-0976.2017.03.002 (2017).
23. Wang, Q. C., Zhang, Y., Yang, Y. H., Yang, W. L. & Li, J. Sequence stratigraphic and lithofacies distributions of Majiagou Formation in Ordos Basin. *J. Northw. Univer. (Nat. Sci. Edn.)* **48**(4), 568–577. https://doi.org/10.16152/j.cnki.xdxbzr.2018-04-012 (2018).
24. Zhao, Z. Y., Sun, Y. S., Li, C. S. & Zhang, Q. Stratigraphic division and correlation of Ordovician system in Ordos Basin. *Special Oil Gas Reser.* **22**(5), 9–17. https://doi.org/10.3969/j.issn.1006-6535.2015.05.002 (2015).
25. Zhang, Y. D. et al. Ordovician integrative stratigraphy and timescale of China. *Sci. China Earth Sci.* **62**, 61–88. https://doi.org/10.1007/s11430-017-9279-0 (2019).
26. Cocks, L. R. M. & Torsvik, T. H. Ordovician palaeogeography and climate change. *Gondwana Res.* **100**, 53–72. https://doi.org/10.1016/j.gr.2020.09.008 (2021).
27. Taylor, S. R. & Mclennan, S. M. *An examination of the geochemical record preserved in sedimentary rocks. The continental crust: Its composition and evolution* (Blackwell Scientific Publications, 1985).
28. Algeo, T. J. & Tribovillard, N. Environmental analysis of paleoceanographic systems based on molybdenum–uranium covariation. *Chem. Geol.* **268**(3/4), 211–225. https://doi.org/10.1016/j.chemgeo.2009.09.001 (2009).
29. Piper, D. Z. & Perkins, R. B. A modern vs. Permian black shale-the hydrography, primary productivity, and water-column chemistry of deposition. *Chem. Geol.* **206**(3/4), 177–197. https://doi.org/10.1016/j.chemgeo.2003.12.006 (2004).
30. Morford, J. L., Emerson, S. R., Breckel, E. J. & Kim, S. H. Diagenesis of oxyanions (V, U, Re, and Mo) in pore waters and sediments from a continental margin. *Geochim. Cosmochim. Acta* **69**(21), 5021–5032. https://doi.org/10.1016/j.gca.2005.05.015 (2005).
31. Tribovillard, N., Algeo, T. J., Lyons, T. & Riboulleau, A. Trace metals as paleoredox and paleoproductivity proxies: An update. *Chem. Geol.* **232**(1/2), 12–32. https://doi.org/10.1016/j.chemgeo.2006.02.012 (2006).
32. Chang, H. J., Chu, X. L., Feng, L. J., Huang, J. & Zhang, Q. R. Redox sensitive trace elements as paleoenvironments proxies. *Geol. Rev.* **55**(1), 91–99. https://doi.org/10.16509/j.georeview.2009.01.01 (2009).
33. Zhang, M. L. et al. New progress on geochemical indicators of ancient oceanic redox condition. *Geol. Sci. Technol. Inform.* **36**(4), 95–106. https://doi.org/10.19509/j.cnki.dzkq.2017.0412 (2017).
34. Taylor, S. R., Mclennan, S. M., Armstrong, R. L. & Tarney, J. The composition and evolution of the continental crust: Rare earth element evidence from sedimentary rocks [and discussion]. *Phil. Trans. R. Soc. Lond. A* **301**, 381–399. https://doi.org/10.1098/rsta.1981.0119 (1981).
35. Webb, G. E. & Kamber, B. S. Rare earth elements in Holocene reefal microbialites: A new shallow seawater proxy. *Geochim. Cosmochim. Acta* **64**(9), 1557–1565. https://doi.org/10.1016/S0016-7037(99)00400-7 (2000).
36. Zhang, P., Hua, H. & Liu, W. G. Isotopic and REE evidence for the paleoenvironmental evolution of the late Ediacaran Denying section, Ningqiang of Shaanxi province, China. *Precambrian Res.* **242**, 96–111. https://doi.org/10.1016/j.precamres.2013.12.011 (2014).
37. Banner, J. L., Hanson, C. N. & Meyers, W. J. Rare-earth element and Nd isotopic variations in regionally extensive dolomites from the Burlington-Keokuk Formation (Mississippian); Implications for REE mobility during carbonate diagenesis. *J. Sediment. Res.* **58**(3), 415–432. https://doi.org/10.1306/212F8DAA-2B24-11D7-8648000102C1865D (1988).
38. Prasanta, K. M. & Sarada, P. M. Geochemistry of carbonate rocks of the Chilpi Group, Bastar Craton, India: Implications on ocean paleoredox conditions at the late Paleoproterozoic Era. *Precambr. Res.* **353**, 106023. https://doi.org/10.1016/j.precamres.2020.106023 (2021).
39. Bolhar, R., Kamber, B. S., Moorbath, S., Fedo, C. M. & Whitehouse, M. J. Characterisation of early Archaean chemical sediments by trace element signatures. *Earth Planet. Sci. Lett.* **222**, 43–60. https://doi.org/10.1016/j.epsl.2004.02.016 (2004).
40. Sarangi, S., Mohanty, S. P. & Barik, A. Rare earth element characteristics of Paleoproterozoic cap carbonates pertaining to the Sausar Group, Central India: Implications for ocean paleoredox conditions. *J. Asian Earth Sci.* **148**, 31–50. https://doi.org/10.1016/j.jseaes.2017.08.016 (2017).
41. Tribovillard, N., Algeo, T. J., Baudin, F. & Riboulleau, A. Analysis of marine environmental conditions based on molybdenum-uranium covariation-Applications to Mesozoic paleoceanography. *Chem. Geol.* **324–325**, 46–58. https://doi.org/10.1016/j.chemgeo.2011.09.009 (2012).
42. Algeo, T. J. & Lyons, T. W. Mo-total organic carbon covariation in modern anoxic marine environments: Implications for analysis of paleoredox and paleohydrographic conditions. *Paleoceanography* **21**(1), 1–23. https://doi.org/10.1029/2004pa001112 (2006).
43. Tang, D. J., Shi, X. Y., Zhao, X. K., Wang, X. Q. & Song, G. Y. Mo-U covariation as an important proxy for sedimentary environment redox conditions-Progress. *Probl Prospects, Geosci.* **29**(1), 1–13. https://doi.org/10.3969/j.issn.1000-8527.2015.01.001 (2015).
44. Sarkar, A., Sarangi, S., Ebihara, A., Bhattacharya, S. K. & Ray, A. K. Carbonate geochemistry across the Eocene/Oligocene Boundary of Kutch, Western India: Implications to oceanic O_2-poor condition and foraminiferal extinction. *Chem. Geol.* **201**(3–4), 281–293. https://doi.org/10.1016/S0009-2541(03)00238-9 (2003).
45. Ren, Y. et al. The paleoenvironmental evolution of the Cambrian Longwangmiao Formation (stage 4, Toyonian) on the Yangtze platform, South China: Petrographic and geochemical constrains. *Mar. Pet. Geol.* **100**, 391–411. https://doi.org/10.1016/j.marpetgeo.2018.10.022 (2019).
46. Derryl, A., Kaufman, A. J. & Jacobsen, S. B. Sedimentary cycling and environmental change in the Late Proterozoic: Evidence from stable and radiogenic isotopes. *Geochim. Cosmochim. Acta* **56**(3), 1317–1329. https://doi.org/10.1016/0016-7037(92)90064-P (1992).
47. Jacobsen, S. B. & Kaufman, A. J. The Sr, C and O isotopic evolution of Neoproterozoic seawater. *Chem. Geol.* **161**(1/3), 37–57. https://doi.org/10.1016/S0009-2541(99)00080-7 (1999).
48. Algeo, T. J. & Maynard, J. B. Trace element behavior and redox facies in core shales of Upper Pennsylvanian Kansas-type cyclothems. *Chem. Geol.* **206**(3/4), 289–318. https://doi.org/10.1016/j.chemgeo.2003.12.009 (2004).
49. Demaison, G. T. & Moore, G. T. Anoxic environments and oil source bed genesis. *Org. Geochem.* **2**(1), 9–31. https://doi.org/10.1016/0146-6380(80)90017-0 (1980).
50. Chen, C. et al. The geochemical characteristics and factors controlling the organic matter accumulation of the Late Ordovician-Early Silurian black shale in the Upper Yangtze Basin, South China. *Marine Petrol. Geol.* **76**, 159–175. https://doi.org/10.1016/j.marpetgeo.2016.04.022 (2016).
51. Hatch, J. R. & Leventhal, J. S. Relationship between inferred redox potential of the depositional environment and geochemistry of the Upper Pennsylvanian (Missourian) Stark Shale Member of the Dennis limestone, Wabaunsee County, Kansas, USA. *Chem Geol* **99**, 65–82. https://doi.org/10.1016/0009-2541(92)90031-Y (1992).
52. Jones, B. & Manning, D. A. C. Comparison of geochemical indices used for the interpretation of palaeoredox conditions in ancient mudstones. *Chem. Geol.* **114**, 111–129. https://doi.org/10.1016/0009-2541(94)90085-X (1994).
53. Liu, X. M., Hardisty, D. S., Lyons, T. W. & Swart, P. K. Evaluating the fidelity of the cerium paleoredox tracer during variable carbonate diagenesis on the Great Bahamas Bank. *Geochim. Cosmochim. Acta* **248**, 25–42. https://doi.org/10.1016/j.gca.2018.12.028 (2019).
54. Bai, S. L., Bai, Z. Q., Ma, X. P., Wang, D. R. & Sun, Y. L. *Ce/La ratio as marker of paleoredox Devonian events and biostratigraphy of South China* (Peking University Press, 1994).
55. Zheng, Y., Anderson, R. F., Van Geen, A. & Fleisher, M. Q. Preservation of non-lithogenic particulate uranium in marine sediments. *Geochim. Cosmochim. Acta* **66**(17), 3085–3092. https://doi.org/10.1016/S0016-7037(01)00632-9 (2002).
56. Mclennan, S. M. Weathering and global denudation. *J. Geol.* **101**(2), 295–303. https://doi.org/10.1086/648222 (1993).

57. Fedo, C. M., Nesbitt, H. W. & Young, G. M. Unraveling the effects of potassium metasomatism in sedimentary rocks and paleosols, with implications for paleoweathering conditions and provenance. *Geology* **23**(10), 921–924. https://doi.org/10.1130/0091-7613(1995)0232.3.CO;2 (1995).
58. Sensarma, S., Rajamani, V. & Tripathi, J. K. Petrography and geochemical characteristics of the sediments of the small River Hemavati, southern India: Implications for provenance and weathering processes. *Sed. Geol.* **205**(3/4), 111–125. https://doi.org/10.1016/j.sedgeo.2008.02.001 (2008).
59. Moradi, A. V., Sari, A. & Akkaya, P. Geochemistry of the Miocene oil shale (Hançili Formation) in the Çankırı-Çorum Basin, Central Turkey: Implications for Paleoclimate conditions, source–area weathering, provenance and tectonic setting. *Sed. Geol.* **341**, 289–303. https://doi.org/10.1016/j.sedgeo.2016.05.002 (2016).
60. Worash, G. Geochemistry provenance and depositional tectonic setting of the Adigrat Sandstone northern Ethiopia. *J. Afr. Earth Sc.* **35**, 185–198. https://doi.org/10.1016/S0899-5362(02)00126-4 (2002).
61. Wu, Y., Du, G. C. & Ma, M. Geochemical characteristics of the sandstones of the Yanchang Formation in the Xunyi area southern Ordos Basin. *Nat. Gas Geosci.* **34**(2), 194–209. https://doi.org/10.11764/j.issn.1672-1926.2022.10.003 (2023).
62. Keith, M. L. & Weber, J. N. Carbon and oxygen isotopic composition of selected limestones and fossils. *Geochem. et Cosmochem. Acta* **18**, 1787–1816. https://doi.org/10.1016/0016-7037(64)90022-5 (1964).
63. Vasconcelos, C., McKenzie, J. A., Warthmann, R. & Bernasconi, S. Calibration of the $\delta^{18}O$ paleo-thermometer with dolomite formed in microbial cultures and natural environments. *Geology* **33**, 317–320. https://doi.org/10.1130/G20992.1 (2005).
64. Grossman, E. L. Chapter 10-Oxygen isotope stratigraphy. *Geol Time Scale* https://doi.org/10.1016/B978-0-444-59425-9.00010-X (2012).
65. Zhang, X. L. Relationship between carbon and oxygen stable isotope in carbonate rocks and paleosalinity and paleotemperature of seawater. *Acta Sedimentol. Sinica* **3**(4), 17–30. https://doi.org/10.14027/j.cnki.cjxb.1985.04.002 (1985).
66. Hays, P. D. & Grossman, E. L. Oxygen isotopes in meteoric calcite cements as indicators of continental paleoclimate. *Geology* **19**(5), 441–444. https://doi.org/10.1130/0091-7613(1991)0192.3.CO;2 (1991).
67. Li, B.Q. Characteristic and identification of diagenetic facies of low permeability and ultra-low permeability dolostone reservoirs: a case study from Ma55 to Ma51 submembers of the Majiagou Formation, central-eastern Ordos Basin. Thesis, Northwest University, pp. 1–175 (in Chinese) (2020).
68. Albanesi, G. L., Barnes, C. R., Trotter, J. A. & Williams, I. S. Comparative lower-middle ordovician conodont oxygen isotope palaeothermometry of the Argentine Precordillera and Laurentian margins. *Palaeogeogr. Palaeoclimatol. Palaeoecol.* **549**, 1–13. https://doi.org/10.1016/j.palaeo.2019.03.016 (2020).
69. Trotter, J. A., Williams, I. S., Barnes, C. R., Lécuyer, C. & Nicoll, R. S. Did cooling oceans trigger Ordovician biodiversification? Evidence from conodont thermometry. *Science* **321**(5888), 550–554. https://doi.org/10.1126/science.1155814 (2008).
70. Hunt, J. M. *Petroleum geochemistry and geology* (W.H. Freeman, 1996).
71. Qin, J. Z. et al. Discussion on the evaluation standards of carbonate source rocks. *Petrol. Geol. Exp.* **26**(3), 281–286. https://doi.org/10.11781/sysydz200403281 (2004).
72. Qin, J. Z. et al. Hydrocarbon-forming organisms and dynamic evaluation of hydrocarbon generation capacity in excellent source rocks. *Petrol. Geol. Exp.* **36**(4), 465–472. https://doi.org/10.11781/sysydz2014044653 (2014).
73. Cao, H. X. et al. Characteristics of carbon and oxygen isotopes of carbonate rocks in Majiagou Formation and their implication, southeastern Ordos Basin. *J. Northw. Univer. (Nat. Sci. Edn.)* **48**(4), 578–586. https://doi.org/10.16152/j.cnki.xdxbzr.2018-04-013 (2018).
74. Wang, Q. C., Gong, X. & Xiao, L. Lithofacies and carbon and oxygen stable isotopic features of Lower Paleozoic limestone in Ordos Basin. *Acta Sedimentol Sinica* **31**(4), 580–589. https://doi.org/10.14027/j.cnki.cjxb.2013.04.019 (2013).
75. Li, Y. N. et al. Potential causes of depleted δ13Ccarb excursions in Ordovician marine carbonates, Ordos Basin, China. *Marine Petrol. Geol.* **134**, 105331. https://doi.org/10.1016/j.marpetgeo.2021.105331 (2021).
76. Ren, Z. L. et al. Thermal history and its controls on oil and gas of the Ordos Basin. *Earth Sci. Front.* **24**(3), 137–148. https://doi.org/10.13745/j.esf.2017.03.012 (2017).
77. Giles, P. S. Low-latitude ordovician to triassic brachiopod habitat temperature (BHTs) determined from $\delta^{18}O_{[brachiopod\ calcite]}$: A cold hard look at ice-house tropical oceans. *Palaeogeogr. Palaeoclimatol. Palaeoecol.* **317–318**(12), 134–152. https://doi.org/10.1016/j.palaeo.2012.01.002 (2012).
78. Abasaghi, F. & Omidpour, A. Geochemical signatures and chemostratigraphic framework for the Early-Middle Permian sedimentary successions of Alborz, Iran. *J. Asian Earth Sci.* **288**, 106607. https://doi.org/10.1016/j.jseaes.2025.106607 (2025).

Author contributions

Yiran Wang: Investigation, Conceptualization, Formal analysis, Writing—original draft, Writing—review & editing. Xiaofeng Wang: Conceptualization, Resources, Supervision, Writing—review & editing. Wenhui Liu: Methodology, Writing—review & editing. Dongdong Zhang and TZ: Conceptualization, Methodology, Investigation. All authors read and approved the final manuscript.

Declarations

Competing interests

The authors declare no competing interests.

Additional information

Supplementary Information The online version contains supplementary material available at https://doi.org/10.1038/s41598-025-12064-w.

Correspondence and requests for materials should be addressed to X.W.

Reprints and permissions information is available at www.nature.com/reprints.

Publisher's note Springer Nature remains neutral with regard to jurisdictional claims in published maps and institutional affiliations.

Open Access This article is licensed under a Creative Commons Attribution-NonCommercial-NoDerivatives 4.0 International License, which permits any non-commercial use, sharing, distribution and reproduction in any medium or format, as long as you give appropriate credit to the original author(s) and the source, provide a link to the Creative Commons licence, and indicate if you modified the licensed material. You do not have permission under this licence to share adapted material derived from this article or parts of it. The images or other third party material in this article are included in the article's Creative Commons licence, unless indicated otherwise in a credit line to the material. If material is not included in the article's Creative Commons licence and your intended use is not permitted by statutory regulation or exceeds the permitted use, you will need to obtain permission directly from the copyright holder. To view a copy of this licence, visit http://creativecommons.org/licenses/by-nc-nd/4.0/.

© The Author(s) 2025